16. Internationales Forum für den lichttechnischen Nachwuchs
Ilmenau, 23. – 25. Juni 2023
DOI (proceedings): 10.22032/dbt.55787

DOI: 10.22032/dbt.58584

Simulative Development of the Electronic Component of Mössbauer Spectroscopy with a Focus on the Controllability of a 2nd Order Transimpedance Amplifier

M.Beyki[1,2,*], J.Pawlak[1,*], R.Patzke[2], and F.Renz[1]
[1]Institute of Inorganic Chemistry, Leibniz University Hanover, Callinstraße 9, D-30167 Hanover, Germany
[2]Faculty I – Electrical Engineering and Information Technology, Hanover University of Applied Sciences and Arts, Ricklinger Stadtweg 120, D-30459 Hanover, Germany

*mohammad.beyki@hs-hannover.de, franz.renz@acd.uni-hannover.de

Keywords: *Transimpedance Amplifier, Photodiode Amplifier, light processing systems*

Topic: *Mössbauer spectroscopy electronic signal amplifier, Transimpedance Amplifier*

Abstract

In light-processing systems, light energy is converted into a photocurrent due to the photoelectric effect. This project focuses on the development of a high-precision energy-to-voltage conversion technique to optimize signal processing in light-processing systems, specifically for applications in space analytics or solid state physikcs, such as Mössbauer spectroscopy. Analog circuit development plays a vital role as downstream voltage conversion is necessary for signal processing. The objective is to enhance the signal quality and improve the signal-to-noise ratio through the design, optimization, and comparison of various circuits for voltage conversion. The development process involves the design and optimization of amplifier circuits, supplemented with the incorporation of filters and/or regulators for further improvement. A transimpedance amplifier is approximated as a second-order low-pass filter, while a state controller is designed and analyzed to efficient transient oscillation of the system towards optimal amplitude values for subsequent signal processing. The project's results contribute to the advancement of light-processing systems, enabling more precise analysis of light energy in Mössbauer spectroscopy. The findings are presented in a series of scientific publications, showcasing the effectiveness of the developed circuits and their impact on signal quality. Future work could focus on further optimization and validation of the circuits in real-world applications to confirm their performance and reliability. Overall, this project emphasizes the significance of meticulous circuit development and optimization for enhancing signal processing in light-processing systems, thus supporting their application in space analytics.

1 Introduction

As extraterrestrial application, the miniaturized Mössbauer spectrometer MIMOS II was very successful on the planet Mars as part of the NASA Mars exploration rover mission Spirit and Opportunity, as IDD payload. “Mössbauer spectra measured on Mars by the Spirit rover during the primary mission are characterized by two ferrous iron doublets (olivine and probably pyroxene) […].” “The ubiquitous presence of olivine in soil suggests that physical rather than chemical weathering processes currently dominate at Gusev crater.” [1]. For this reason the MIMOS II (miniaturized Mössbauer spectrometer) serves as a proven and reliable measuring instrument [2][3]. Detected gamma rays are converted into a current pulse by a PIN diode and converted into a usable output voltage via an amplifier board located behind it [2][3]. MIMOS originally devised by Göstar Klingelhöfer, is further developed by the Renz group at the Leibniz University Hanover in cooperation with the Hanover University of Applied Sciences and Arts [2][4]. In this context here, the transmission behavior of the initially simulated amplifier circuit is to be determined. It serves as a basis for a later control, with which the circuit is to be improved regarding its dynamics [4]. A special focus is placed on the operational amplifier in the circuit analysis [4][5]. This is examined with regard to its amplification characteristics [4].

2 The Amplifier

A transimpedance amplifier (TIA) is an electronic circuit which converts the input current, the so-called photocurrent $i_{\mathrm{ph}}(t)$, into an output voltage $u_{\mathrm{a}}(t)$ is converted. In principle, a linear relationship between $i_{\mathrm{ph}}(t)$ and $u_{\mathrm{a}}(t)$ is assumed [5][6][7].

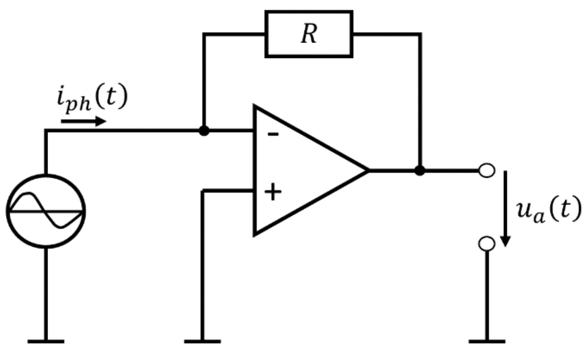

Figure 1: Basic presentation of a Transimpedance Amplifier

- $i_{\mathrm{ph}}(t)$: Photocurrent
- $u_{\mathrm{a}}(t)$: Output Voltage
- R: Negative feedback resistor

$$\underline{U}_{\mathrm{a}}(j\omega) = -R \cdot \underline{I}_{\mathrm{ph}}(j\omega) \tag{2.1}$$

2.1 First Order TIA

The transimpedance amplifier is already known from previous publications. So far, the system description is available in the Fourier or Laplace domain as a low-pass filter of first and second order [4][5][6]. Figure 2 shows the previously published version of the extended 1st order transimpedance amplifier [4][6]. It must be mentioned here that the input impedance $\underline{Z}_{\mathrm{in}}(j\omega)$, the maximum open-circuit voltage gain A_0 and the transit frequency f_{T} of the amplifier must be infinitely high in order to create the optimal conditions for the previous mathematical description. In application, however, it turns out that often a parallel capacitor C to the negative feedback resistor R has to filter out high frequency components. This results in a low-pass characteristic, which can be described [5][6][7]:

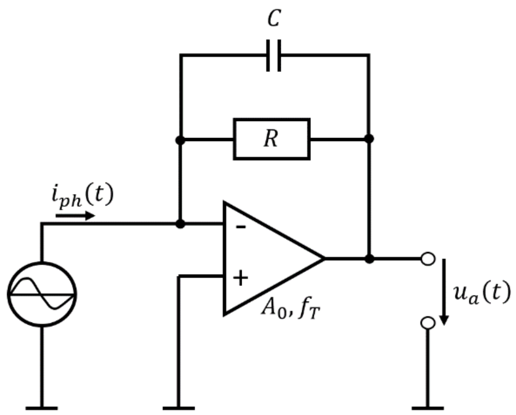

Figure 2: TIA with capacitive feedback

- $i_{\mathrm{ph}}(t)$: Photocurrent
- $u_{\mathrm{a}}(t)$: Output Voltage
- R: Negative feedback resistor
- C: Parallel capacitance
- f_{T}: Transit frequency
- A_0: Maximum open circuit voltage gain of the TIA

$$\underline{U}_a(j\omega) = \frac{-R}{1 + j\omega RC} \cdot \underline{I}_{\mathrm{ph}}(j\omega) \tag{2.2}$$

In order to create a better overview with regard to the mathematical modeling, the Fourier representation is changed to the Laplacian representation.

$$U_{\mathrm{a}}(s) = \frac{-R}{1 + s \cdot RC} \cdot I_{\mathrm{ph}}(s) \tag{2.3}$$

Since only the transmission behavior is relevant, now follows a transition in the required mathematical direction:

$$G(s) = \frac{U_{\mathrm{a}}(s)}{I_{\mathrm{ph}}(s)} = \frac{-R}{1 + s \cdot RC} \tag{2.4}$$

2.2 Second Order TIA

Figure 3 shows an extension of the previous circuits of the TIA to extend the system order of the mathematical description of the transmission behavior to $n = 2$ [4][5][6][7].

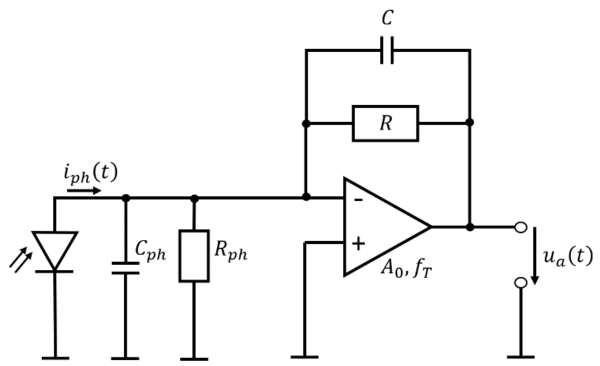

Figure 3: Transimpedance Amplifier for 2nd Order Description

- $i_{\mathrm{ph}}(t)$: Photocurrent
- $u_{\mathrm{a}}(t)$: Output Voltage
- R: Negative feedback resistor
- C: Parallel capacitance
- f_{T}: Transit frequency
- A_0: Maximum open circuit voltage gain of the TIA
- C_{ph}: Parallel capacitance of the diode
- R_{ph}: Parallel resistance of the diode

$$G(s) = \frac{U_{\mathrm{a}}(s)}{I_{\mathrm{ph}}(s)} \approx \frac{K_{\mathrm{P}} \cdot (\omega_0)^2}{s^2 + 2 \cdot D \cdot \omega_0 \cdot s + (\omega_0)^2} \tag{2.5}$$

$$\ddot{u}_{\mathrm{a}}(t) + 2 \cdot D \cdot \omega_0 \cdot \dot{u}_{\mathrm{a}}(t) + (\omega_0)^2 \cdot u_{\mathrm{a}}(t) = K_{\mathrm{P}} \cdot (\omega_0)^2 \cdot i_{\mathrm{ph}}(t) \tag{2.6}$$

The step response of the system is shown in figure 4.

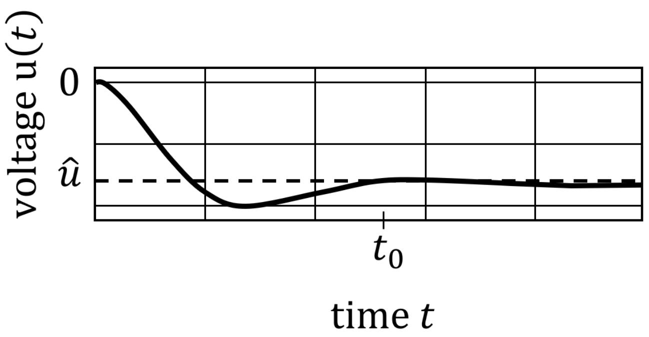

Figure 4: Step Response of the System

3 State Space Description

In the state space, stability and controllability can each be studied independently and a state controller can be designed. Unlike conventional controllers, which can only take a single signal variable to influence the output of a system, state controllers are used to influence the output of a system and to utilize multiple state variables in the signal recording for this purpose. That is, if the distance y is to be influenced, both distance values and velocity values are used for the controller design. This increases the possibility of the influence enormously and leads with suitable execution of the method to a better result in relation to the control [4][9][10].

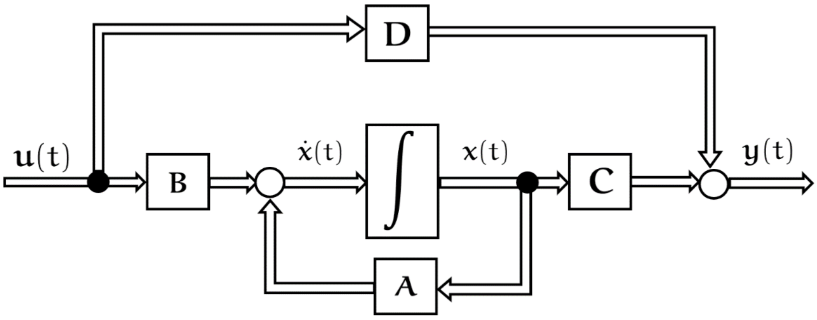

Figure 5: Standardized Blockdiagram of the State Space Description

Figure 5 shows a standardized block diagram of a system in the state space. In order to specify a system in the state space, we first define the states and inputs of the system are defined. The states x_{i} are summarized in the state vector $\boldsymbol{x}(t)$ and the inputs u_{i} in the input vector $\boldsymbol{u}(t)$ [4][9][10].

$$\boldsymbol{x}(t) = \begin{pmatrix} x_1 \\ x_2 \\ \vdots \\ x_{\mathrm{n}} \end{pmatrix}, \qquad \boldsymbol{u}(t) = \begin{pmatrix} u_1 \\ u_2 \\ \vdots \\ u_{\mathrm{m}} \end{pmatrix}$$

The relationship between the states and the inputs is:

$$\dot{\boldsymbol{x}}(t) = \boldsymbol{A} \cdot \boldsymbol{x}(t) + \boldsymbol{B} \cdot \boldsymbol{u}(t) \tag{3.1}$$

The outputs are specified as follows:

$$\boldsymbol{y}(t) = \boldsymbol{C} \cdot \boldsymbol{x}(t) + \boldsymbol{D} \cdot \boldsymbol{u}(t) \tag{3.2}$$

The system matrix $\boldsymbol{A}$ can take many different forms, the only important thing is that the correlation information between the differentiations $\dot{x}_{\mathrm{i}}$ and the non-differential states x_{i} are in a unique relationship and the influence of the inputs u_{i} is represented by means of the input matrix $\boldsymbol{B}$ which adjusts in each case. The outputs y_{i} are defined by the output state matrix $\boldsymbol{C}$ and the direct relationship between inputs u_{i} and outputs y_{i} $\boldsymbol{D}$ [4].

$$u_{\mathrm{a}} = x_1, \qquad \dot{x}_1 = x_2$$

$$\boldsymbol{A} = \begin{bmatrix} 0 & 1 \\ -(\omega_0)^2 & -2 \cdot D \cdot \omega_0 \end{bmatrix} \tag{3.3}$$

$$\boldsymbol{b} = \begin{bmatrix} 0 \\ K_\mathrm{P} \cdot (\omega_0)^2 \end{bmatrix} \tag{3.4}$$

$$\boldsymbol{c}^\mathrm{T} = \begin{bmatrix} 0 & 1 \end{bmatrix} \tag{3.5}$$

$$\begin{bmatrix} \dot{x}_1(t) \\ \dot{x}_2(t) \end{bmatrix} = \begin{bmatrix} 0 & 1 \\ -(\omega_0)^2 & -2 \cdot D \cdot \omega_0 \end{bmatrix} \cdot \begin{bmatrix} x_1(t) \\ x_2(t) \end{bmatrix} + \begin{bmatrix} 0 \\ K_\mathrm{P} \cdot (\omega_0)^2 \end{bmatrix} \cdot u(t) \tag{3.6}$$

$$y(t) = \begin{bmatrix} 0 & 1 \end{bmatrix} \cdot \begin{bmatrix} x_1(t) \\ x_2(t) \end{bmatrix} \tag{3.7}$$

3.1 Stability and Controllability in the State Space

The stability and controllability of a system are basic requirements for good control. For this reason, both aspects of a system must be illuminated in each case. First, the stability of the system is considered in more detail and set up for each state. This is followed by a controllability analysis, also related to each individual state. Only after these investigations a controller design can be made and the state controller **K** be determined so that each state can be controlled and so each eigenvalue shifted to a favourable position.

3.1.1 Stability in the State Space

The stability of the system is defined by the eigenvalues λ_i of the system matrix $\boldsymbol{A}$. If these eigenvalues all have a negative real part, the system is stable [8][9][10].

$$Re\{\lambda_\mathrm{i}\} < 0, \qquad \mathrm{i} = 1, \dots \mathrm{n}$$

If almost all eigenvalues are in the left half plane and one eigenvalue is on the imaginary axis, the system is limit stable.

$$Re\{\lambda_\mathrm{i}\} < 0, \qquad \mathrm{i} = 1, \dots \mathrm{n} - 1, \qquad Re\{\lambda_\mathrm{n}\} = 0$$

All other cases indicate an unstable system.

$$\det(\lambda \cdot \boldsymbol{I} - \boldsymbol{A}) = 0$$

$$\begin{vmatrix} \lambda & -1 \\ (\omega_0)^2 & \lambda + 2D\omega_0 \end{vmatrix} = \lambda^2 + 2D\omega_0\lambda + (\omega_0)^2 = 0 \tag{3.8}$$

$$\lambda_{1,2} = -D\omega_0 \pm \omega_0\sqrt{D^2 - 1} = -D\omega_0 \pm j\omega_0\sqrt{1 - D^2} \tag{3.9}$$

$$\lambda_{1,2} = \delta \pm j\omega_\mathrm{d} \tag{3.10}$$

$$\delta = -D\omega_0 \tag{3.11}$$

$$\omega_\mathrm{d} = \omega_0\sqrt{1-D^2} \tag{3.12}$$

Due to the fact that the real part of the eigenvalues λ_i is negative

$$Re\{\lambda_\mathrm{i}\} = \delta = -D\omega_0 < 0, \ \{D, \omega_0\} > 0,$$

it is a fully stable system.

3.1.2 Controllability in the State Space

The controllability of a system is defined by the controllability matrix $\boldsymbol{Q}_\mathrm{S}$. If this matrix has full rank, controllability exists. Alternatively, the determinant of the controllability matrix can be formed for quadratic matrices [4][9][10].

$$\boldsymbol{Q}_\mathrm{S} = [\boldsymbol{B} \quad \boldsymbol{A}\cdot\boldsymbol{B} \quad \boldsymbol{A}^2\cdot\boldsymbol{B} \quad \dots \quad \boldsymbol{A}^{n-1}\cdot\boldsymbol{B}] \tag{3.13}$$

$$\mathrm{rank}(\boldsymbol{Q}_\mathrm{S}) = n, \qquad \det(\boldsymbol{Q}_\mathrm{S}) \neq 0$$

n indicates the system order and is thus to be taken as an indicator of full rank.

$$\boldsymbol{Q}_\mathrm{S} = \begin{bmatrix} 0 & K_\mathrm{P}\cdot(\omega_0)^2 \\ K_\mathrm{P}\cdot(\omega_0)^2 & -2\cdot D\cdot(\omega_0)^3\cdot K_\mathrm{P} \end{bmatrix} \tag{3.13}$$

$$\det(\boldsymbol{Q}_\mathrm{S}) = [-(K_\mathrm{P}\cdot\omega_0^2)^2] \neq 0 \tag{3.14}$$

Since each state x_i is controllable, there is complete controllability of the entire system, so that by means of a state controller $\boldsymbol{K}$ each eigenvalue of the system can be shifted to a position favourable for operational purposes. For this reason, the state controller $\boldsymbol{K}$ is designed in the next section. The method of Ackermann is used to achieve a system speed and accuracy that is favorable for operational purposes.

4 The Controller

The state space model or description of the system (fig. 4) opens up a whole range of further and, above all, multidimensional control options. The state controller $\boldsymbol{K}$ feeds back each state under scalar change and in this way it shifts the eigenvalues of the system (fig. 6).

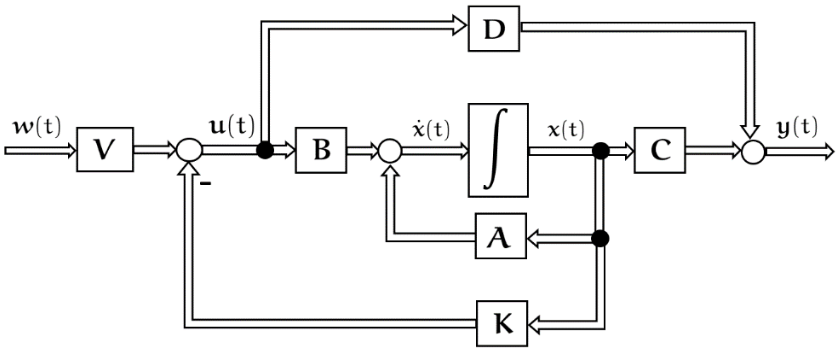

*Figure 6: State Space Model and State Controller **K***

4.1 Ackermann Method

In the continuous case, Ackermann's pole specification is used to determine a feedback vector $\boldsymbol{k}^{\mathrm{T}}$ in the state space. For this purpose, in the first step a controllability analysis as in the previous section has to be done. Usually the determinant of the controllability matrix $\boldsymbol{Q}_{\mathrm{S}}$ according to Kalman is sufficient. Since the system has only one input signal, it is sufficient to design $\boldsymbol{K}$ as a singlerow control vector $\boldsymbol{K} \rightarrow \boldsymbol{k}^{\mathrm{T}}$ and $\boldsymbol{V}$ becomes a scalar value $\boldsymbol{V} \rightarrow \mathrm{v}$. The feed forward control v of the system is used to scale the output signal as desired. Mostly v is used to normalize the step response of the controlled system to the value one. Using Ackermann's method, new poles $\tilde{s}_{\mathrm{p,i}}$ can be specified for the system dynamics of the controlled system. [9][10].

$$\Pi_{i=1}^{n}\left(\mathrm{s} - \tilde{s}_{\mathrm{p},i}\right) = \alpha_0 + \alpha_1 \cdot s + \alpha_2 \cdot s^2 + \dots + \alpha_{\mathrm{n}-1} \cdot s^{\mathrm{n}-1} + s^{\mathrm{n}} \tag{4.1}$$

$$\boldsymbol{Q}_{\mathrm{S}} = [\boldsymbol{B} \quad \boldsymbol{A} \cdot \boldsymbol{B} \quad \boldsymbol{A}^2 \cdot \boldsymbol{B} \quad \dots \quad \boldsymbol{A}^{n-1} \cdot \boldsymbol{B}] \tag{3.13}$$

$$\boldsymbol{t}_1^{\mathrm{T}} = [0 \quad \dots \quad 0 \quad 1] \cdot \boldsymbol{Q}_{\mathrm{S}}^{-1} = [\boldsymbol{0} \quad 1] \cdot \boldsymbol{Q}_{\mathrm{S}}^{-1} \tag{4.2}$$

$$\boldsymbol{P}_{\alpha}(\boldsymbol{A}) = \sum_{k=o}^{n-1} \alpha_k \cdot \boldsymbol{A}^k = \alpha_0 \cdot \boldsymbol{I} + \alpha_1 \cdot \boldsymbol{A}^1 + \dots + \alpha_{\mathrm{n}-1} \cdot \boldsymbol{A}^{\mathrm{n}-1} + \boldsymbol{A}^{\mathrm{n}} \tag{4.3}$$

$$\boldsymbol{k}^{\mathrm{T}} = \boldsymbol{t}_1^{\mathrm{T}} \cdot \boldsymbol{P}_{\alpha}(\boldsymbol{A}) \tag{4.4}$$

$$\mathrm{v} = [\boldsymbol{c}^{\mathrm{T}} \cdot (\boldsymbol{b} \cdot \boldsymbol{k}^{\mathrm{T}} - \boldsymbol{A})^{-1} \cdot \boldsymbol{b}]^{-1} \tag{4.5}$$

n denotes the system order. $\boldsymbol{P}_{\alpha}(\boldsymbol{A})$ carries in the form of α_{i} the coefficients of the corresponding new characteristic polynomial function together with new pole specification of the system.

4.2 Controller

Applied to the second order system under consideration, it follows:

$$\boldsymbol{Q}_{\mathrm{S}}^{-1} = \begin{bmatrix} * & * \\ \frac{1}{K_{\mathrm{P}} \cdot (\omega_0)^2} & 0 \end{bmatrix} \tag{4.6}$$

$$\boldsymbol{t}_1^{\mathrm{T}} = [\boldsymbol{0} \quad 1] \cdot \boldsymbol{Q}_{\mathrm{S}}^{-1} = \begin{bmatrix} \frac{1}{K_{\mathrm{P}} \cdot (\omega_0)^2} & 0 \end{bmatrix} \tag{4.7}$$

The matrix $\boldsymbol{P}_\alpha(\boldsymbol{A})$ carries the information of the new poles and has to be chosen carefully. In the considered case there is a 2nd order system and only two new poles can be chosen.

$$\begin{aligned} \left(s - \tilde{s}_{\mathrm{p},1}\right) \cdot \left(s - \tilde{s}_{\mathrm{p},2}\right) &= s^2 - \left(\tilde{s}_{\mathrm{p},1} + \tilde{s}_{\mathrm{p},2}\right) \cdot s + \tilde{s}_{\mathrm{p},1} \cdot \tilde{s}_{\mathrm{p},2} \\ &= s^2 + \alpha_1 \cdot s + \alpha_0 \\ \alpha_0 = \tilde{s}_{\mathrm{p},1} \cdot \tilde{s}_{\mathrm{p},2}, \qquad & \alpha_1 = -\left(\tilde{s}_{\mathrm{p},1} + \tilde{s}_{\mathrm{p},2}\right) \end{aligned} \tag{4.8}$$

For the controller, therefore, the following description results for the case under consideration:

$$\begin{aligned} \boldsymbol{k}^{\mathrm{T}} &= \boldsymbol{t}_1^{\mathrm{T}} \cdot \boldsymbol{P}_\alpha(\boldsymbol{A}) = \alpha_0 \cdot \boldsymbol{I} + \alpha_1 \cdot \boldsymbol{A}^1 + \boldsymbol{A}^2 \\ &= \tilde{s}_{\mathrm{p},1} \cdot \tilde{s}_{\mathrm{p},2} \cdot \begin{bmatrix} 1 & 0 \\ 0 & 1 \end{bmatrix} - \left(\tilde{s}_{\mathrm{p},1} + \tilde{s}_{\mathrm{p},2}\right) \cdot \begin{bmatrix} 0 & 1 \\ -(\omega_0)^2 & -2 \cdot D \cdot \omega_0 \end{bmatrix} + \begin{bmatrix} 0 & 1 \\ -(\omega_0)^2 & -2 \cdot D \cdot \omega_0 \end{bmatrix}^2 \end{aligned} \tag{4.9}$$

At this point it is only clear that the new poles must lie on the left side of the complex Laplace plane, otherwise there is no stability. Now it must be decided according to the further application how the exact position of the poles has to be chosen. If the system is to react as fast as possible, a slight overshoot must be expected. If it is not allowed to oscillate, the poles have to be selected differently and may lead to greater delays. Furthermore, the exact dimensioning depends on how much leeway the real implementation offers. For example, capacitors must be selected for any feedbacks. These limit the mathematically possible range on their practicability and lead thereby to deviations from the exactly calculated values of the new poles – it must be urgently paid attention to tolerances. A further influencing factor is the signal noise and can also lead to a strong shift of the poles in case of a rough deviation, sometimes also to instabilities.

The choice of the correct pole position is selected at this point according to how the previous poles are already positioned and how much faster the new system response must look in relation to them. The old response is shown in figure 7.

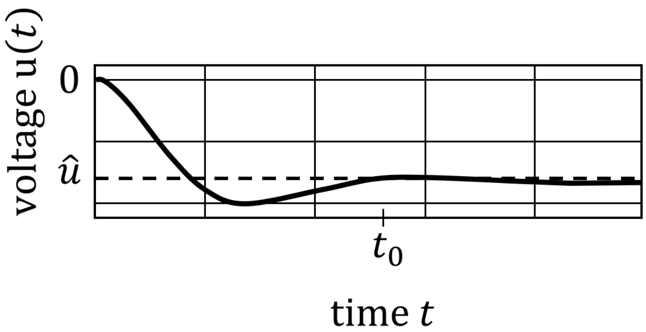

Figure 7: Step Response of the System

In terms of unregulated system response, the new poles are selected so that the system response requires only 57 percent of the old settling time.

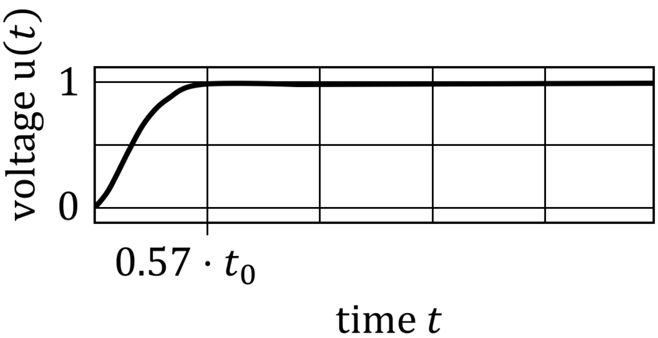

Figure 8: Step Response of the Controlled System

5 Conclusion

In conclusion, this project aimed to develop a high-precision energy-to-voltage conversion technique to enhance signal processing in light-processing systems, specifically for applications in space analytics, such as Mössbauer spectroscopy. Analog circuit development played a crucial role as signal processing could only be performed after downstream voltage conversion. The development primarily focused on amplifier circuits, with the addition of filters and/or regulators for optimization. These enhancements resulted in a significant improvement in the signal-to-noise ratio and overall signal quality. Furthermore, a transimpedance amplifier was approximated as a second-order low-pass filter, while a state controller was specifically designed and further analyzed. The state controller proved instrumental in achieving the system's precise and efficient oscillation towards optimal amplitude values for subsequent signal processing. The outcomes of this project contribute to advancing the performance of light-processing systems and enable more accurate analysis of light energy in Mössbauer spectroscopy. Future work could focus on further optimizing the developed circuits and validating their performance and reliability in real-world applications. Overall, this project underscores the importance of careful circuit development and optimization in improving signal processing quality in light-processing systems, thereby supporting their applications in space analytics.

Acknowledgements

The authors would like to thank Hannover School for Nanotechnology (hsn) Leibniz University Hannover (LUH) Laboratory of Nanotechnology and Quantum Engineering (LNQE), Hanover University of Applied Sciences and Arts (HsH) and the UMB-II project.

References

[1] R. V. Morris, G. Klingelhöfer, B. Bernhart, C. Schröder, D. S. Rodionov, P. A. de Souza, JR., A. Yen, R. Gellert, E. N. Evlanov, J. Foh, E. Kankeleit, P. Gütlich, D. W. Ming, F. Renz, T. Wdowiak, S. W. Squyres, and R. E. Arvidson; SCIENCE ,6 Aug 2004, Vol 305, Issue 5685, pp. 833-836

[2] M. Blumers, B. Bernhardt, P. Lechner, G. Klingelhöfer, C. d'Uston, H. Soltau, L. Strüder, R. Eckerhardt, J. Brückner, H. Henkel, J.G. Lopez, J. Maul, 'The miniaturised Mössbauer spectrometer MIMOS II A: Increased sensitivity and new capability for element alanalysis', Nuclear Instruments and Methods in Physics Research A 624 (2010) 277–281, journalhomepage: www.elsevier.com/locate/nima, 2010

[3] G. Klingelhöfer, B. Fegley, R.V. Morris, E. Kankeleit, P. Held, E. Evlanov, O. Priloutskii, Planetary and Space Science, 44, 11, 1277-1288 (1996).

[4] M. Beyki, J. Pawlak, R. Patzke, F. Renz, 'Simulation of the electronic part of Mössbauer spectroscopy', Proceedings of the 2nd OPU-HsH Japanese-German Symposium 2023: Industry 4.0 and Society 5.0 for Smart Society, DOI: https://doi.org/10.25968/opus-2459, 2023

[5] B. Razavi, 'A CIRCUID FOR ALL SEASONS – The Transimpedance Amplifier', University of California Los Angeles 2019, Los Angeles, USA, http://www.seas.ucla.edu/brweb/papers/Journals/BR_SSCM_1_2019.pdf

[6] X. Ramus, 'Transimpedance Considerations for High-Speed Amplifiers', Texas Instruments: Application Report – SBOA122 November 2009, https://www.ti.com/lit/an/sboa122/sboa122.pdf, 2009

[7] R. Patzke, 'Schnelle und rauscharme Photonenmessung mit pin-Fotodioden', Hochschule Hannover – University of Applied Sciences and Arts, Fachgebiet Integrierte Schaltungen und Eingebettete Systeme (IES), DOI: https://doi.org/10.25968/opus-2315, 31/July/2022

[8] M. Beyki, R. Kutzner, U. Lindemann, 'Systemtheorie & Optimale Regelung – Teil I Einführung in den Zustandsraum', 1st edition, Hochschule Hannover – University of Applied Sciences and Arts, DOI: https://doi.org/10.25968/opus-2441, 2023.

[9] M. Beyki, R. Kutzner, U. Lindemann, 'Systemtheorie & Optimale Regelung – Teil V Zustandsregelung', 1st edition, Hochschule Hannover – University of Applied Sciences and Arts, DOI: https://doi.org/10.25968/opus-2442, 2023.

[10] O. Föllinger, U. Konigorski, B. Lohmann, G. Roppenecker, A. Trächtler, 'Regelungstechnik: Einführung in die Methoden und ihre Anwendung', 13th edition, VDE VERLAG GMBH, 2022, p. 168 – 188.